J Neurophysiol 104: 2886–2899, 2010.
First published September 29, 2010; doi:10.1152/jn.00585.2009.

Speed and Eccentricity Tuning Reveal a Central Role for the Velocity-Based Cue to 3D Visual Motion

Thaddeus B. Czuba,[1] Bas Rokers,[1,2] Alexander C. Huk,[1,2] and Lawrence K. Cormack[1]
[1]*Center for Perceptual Systems, Department of Psychology, Section of Neurobiology,* [2]*The University of Texas at Austin, Austin, Texas*

Submitted 9 July 2009; accepted in final form 22 September 2010

Czuba TB, Rokers B, Huk AC, Cormack LK. Speed and eccentricity tuning reveal a central role for the velocity-based cue to 3D visual motion. *J Neurophysiol* 104: 2886–2899, 2010. First published September 29, 2010; doi:10.1152/jn.00585.2009. Two binocular cues are thought to underlie the visual perception of three-dimensional (3D) motion: a disparity-based cue, which relies on changes in disparity over time, and a velocity-based cue, which relies on interocular velocity differences. The respective building blocks of these cues, instantaneous disparity and retinal motion, exhibit very distinct spatial and temporal signatures. Although these two cues are synchronous in naturally moving objects, disparity-based and velocity-based mechanisms can be dissociated experimentally. We therefore investigated how the relative contributions of these two cues change across a range of viewing conditions. We measured direction-discrimination sensitivity for motion though depth across a wide range of eccentricities and speeds for disparity-based stimuli, velocity-based stimuli, and "full cue" stimuli containing both changing disparities and interocular velocity differences. Surprisingly, the pattern of sensitivity for velocity-based stimuli was nearly identical to that for full cue stimuli across the entire extent of the measured spatiotemporal surface and both were clearly distinct from those for the disparity-based stimuli. These results suggest that for direction discrimination outside the fovea, 3D motion perception primarily relies on the velocity-based cue with little, if any, contribution from the disparity-based cue.

INTRODUCTION

Most research on motion perception has focused on two-dimensional (2D) frontoparallel motion (which is, of course, the easiest to generate on computer-driven displays). The neural computations that support the perception of motion through a more realistic three-dimensional (3D) environment are considerably less well-understood. Here, we explore the relative contributions of two fundamental binocular cues to 3D motion (sometimes referred to as motion-in-depth or *z*-axis stereomotion): one based on changes in binocular disparity over time and one based on interocular velocity differences.[1] We investigated the conditions under which the visual system might preferentially rely on one cue over the other to shed light on how 3D motion is processed by the brain.

The first potential cue, changing disparity over time (CD), is classically assumed to be the pure, fundamental signal for binocular 3D motion perception (Cumming and Parker 1994; Gray and Regan 1996; Regan and Gray 2009). The CD cue can be computed simply by taking the time derivative of horizontal binocular disparity (Fig. 1, *top*). Although this cue is sufficient for the generation of 3D motion percepts, it is important to note that it is based on disparity signals, which are greatly degraded at far eccentricities and high temporal frequencies (e.g., Blakemore 1970; Julesz 1960; Norcia and Tyler 1984; Westheimer and Truong 1988). We therefore hypothesized that the CD cue might preferentially support 3D motion percepts for slowly moving stimuli near fixation.

The second potential cue, the interocular velocity difference (IOVD), has been proposed to also contribute to 3D motion perception (Harris et al. 2008; but see Regan and Gray 2009). The IOVD cue can be computed by comparing monocular velocity signals of the stimulus projections on each of the two retinae (Fig. 1, *bottom*). This computation exploits the fact that motion through depth projects different (and often opposite) motion on the retinae of both left and right eyes. Although the IOVD cue has proven challenging to study in isolation, one might expect it to be perceptually robust across eccentricity and speed, given that it is based on monocular motion signals (e.g., McKee and Nakayama 1984; Wright 1987). We therefore hypothesized that the visual system may rely more heavily on the velocity-based IOVD cue to 3D motion for faster motions outside the fovea—the very conditions under which the disparity-based CD cue might be expected to be relatively ineffective.

To compare the relative contributions of the CD and IOVD cues, we assessed sensitivity with a common task and metric across all conditions. To do this, we asked observers to discriminate the direction of motion of a frontoparallel plane of dots moving toward or away through depth. We varied stimulus strength in a manner akin to prior manipulations of 2D motion coherence (i.e., the proportion of coherently moving dots on the signal plane relative to noise dots moving incoherently through depth; Burr and Santoro 2001; Lankheet et al. 2000; Newsome and Paré 1988; Watamaniuk et al. 1989). *FULL* binocular cue displays contained signal plane dots moving toward or away from the observer in depth (and thus contained both the CD and IOVD cues); *CD* displays contained one-frame lifetime signal plane dots to remove any structured monocular velocity information (Julesz 1971); *IOVD* displays contained binocularly anticorrelated dots to greatly reduce the ability of the visual system to compute disparity (Harris and Rushton 2003; Rokers et al. 2008).[2]

We measured direction-discrimination thresholds for *FULL*, *CD*, and *IOVD* displays across a wide range of speeds and

[1] A percept of motion through depth has been shown to arise from moving objects visible to one eye and camouflaged to the other (Brooks and Gillam 2006b, 2007). This is a dynamic analog of the stereopsis without binocular correlation described by Kaye (1978). Although interesting, this is beyond the scope of the current study.

Address for reprint requests and other correspondence: T. B. Czuba, The University of Texas at Austin, Section of Neurobiology, Center for Perceptual Systems, Department of Psychology, Austin, TX 78712 (E-mail: thad@mail.utexas.edu).

[2] Even though "FULL" is not an acronym, we spell it in all capital letters so it visually groups with the other two condition names.

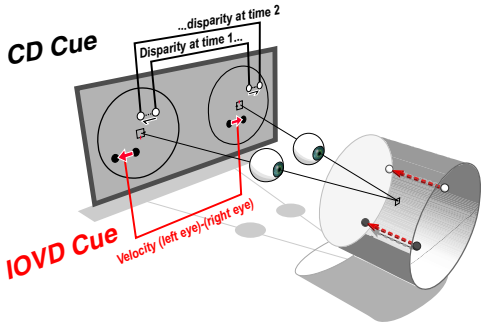

FIG. 1. Binocular cues to three-dimensional (3D) motion. The visual system could infer the direction of 3D motion (white and black spheres moving toward the eyes, in the cylinder at *bottom right*) based on dynamic information from the corresponding two-dimensional (2D) retinal projections (white and black dots, flat panel at *top left*). The schematic depicts 2 known binocular cues to 3D motion. The changing disparity (CD) cue is derived from tracking changes in binocular disparity over time (black brackets and ellipses). The interocular velocity difference (IOVD) cue is derived by comparing monocular velocity signals from corresponding regions in the 2 retinae (red brackets and arrows). Although both cues coexist in natural scenes, experimental stimuli can be used to study the cues together or in isolation (see Fig. 3).

eccentricities. At low speeds, eccentricity degraded sensitivity similarly for all three display types. At faster speeds, however, the relative contributions of the two cues became much more distinct. For the *FULL* and *IOVD* stimuli, sensitivity showed a distinct band-pass speed tuning, with a peak at relatively fast speeds (~2.0°/s monocular velocity). In contrast, sensitivity for the CD stimuli was clearly low-pass; in fact, direction discrimination for these stimuli became impossible at moderately high speeds, regardless of eccentricity.

These results imply that the visual system can compute 3D motion primarily from the IOVD cue across a majority of the visual field for a broad range of speeds and may rely more strongly on the CD cue for direction discrimination at very slow speeds at or near fixation. Although our findings may at first seem to run counter to previous demonstrations that the CD cue is sufficient to explain 3D motion sensitivity (Cumming and Parker 1994; Gray and Regan 1996), our demonstration of the possible primacy of the IOVD cue bolsters a growing, recent literature demonstrating dissociable contributions of the IOVD cue (for a more detailed review, see DISCUSSION and also Harris et al. 2008; Regan and Gray 2009). Furthermore, this relative primacy of IOVDs may result from the fact that our stimulus parameters, discrimination task, and sensitivity metric are better thought of extending the methods used to study 2D/frontoparallel motion processing into the third spatial dimension, as opposed to being temporally dynamic extensions of the methods used to probe disparity-based mechanisms. Finally, the methods introduced herein could easily be generalized for use in future neuroimaging and electrophysiological studies of interocular velocity differences and 3D motion perception.

METHODS

Observers

Data were collected from three experienced psychophysical observers (three of the authors, males, ages 26–44 yr), all with good stereopsis and normal or corrected-to-normal vision. Experiments were undertaken with the written consent of each observer and all procedures were approved by the University of Texas–Austin Institutional Review Board. In all, 156,240 trials were collected across the three observers.

General procedure

We measured the ability of observers to discriminate the direction of motion through depth (directly toward or away from the observer) for three different types of motion cue stimuli (*FULL*, *IOVD*, or *CD*, described more fully in the following text), which contained different combinations of the two primary binocular cues to 3D motion. Performance for each motion cue type was measured in a fully crossed design manipulating stimulus speed and eccentricity. Across all conditions, observers viewed a frontoparallel plane of random dots moving toward or away from them through a 3D volume of noise dots. The signal plane started at a random depth within the volume and moved at a smooth, constant speed either toward or away from the observer, wrapping from front to back (or back to front), to complete one full cycle through the depth volume. The random starting location ensured that the starting, ending, or average disparity (or the time of the wrap) of the plane could not be used to do the task.

On each trial, observers viewed the display and reported the perceived direction of motion through depth (toward or away) with a left or right mouse click. The response triggered the next stimulus presentation, with a minimum delay of 200 ms between trials. Observers were instructed to report their percept of the smoothest motion though depth throughout the experiment, disregarding the perceived jump through depth that occurred when the signal plane wrapped. In all conditions, signal dots were relocated in the x–y plane on z-axis wrapping to minimize apparent motion during this brief change in signal plane depth. No feedback was provided; observers could thus concentrate on the smooth motion and not train themselves (consciously or not) on other potential cues, such as the jump due to wrapping or a utrocular identification combined with a monocular direction judgment.

For each combination of cue type, speed, and eccentricity, we measured the proportion of correct responses as a function of motion coherence, defined as the relative percentage of signal to noise dots. Psychophysical thresholds (84% correct) were then estimated for each condition from a fitted logistic function and sensitivity was expressed as inverse threshold coherence (coh^{-1}). More details about the stimuli and experimental design are provided in the following text.

General stimuli

Observers stereoscopically viewed moving random dot displays in which 80 dark (0.4 cd/m^2) or light (129.7 cd/m^2) binocularly paired dots were presented on a midgray (56.0 cd/m^2) background (Fig. 2*A*). In each monocular half-image, half the dots were dark and half the dots were light. Individual dots subtended a visual angle of 15 arcmin (0.25°) and were antialiased to achieve subpixel position accuracy. Dot density and luminance values were not selected on a single fundamental principle, but rather a balance of several factors. Importantly, we first wanted our stimuli to be comparable to many 2D frontoparallel motion studies that used motion coherence as a manipulation (i.e., number of dots on each display frame [80], stimulus area [126 deg^2], and variable dot lifetimes, resulting in dot densities of 0.7–2.5 dots per degree and 3.7–11.5% dot coverage). We emphasize that many of our stimulus parameters may differ from prior studies of static disparity processing and stereomotion (e.g., lower density). Second, we chose parameters that were within hardware limitations (luminances that fit within the maximum linearized contrast range; dot numbers that did not overstep the available computational power to relocate each signal/noise dot on every display frame). Third, we chose parameters that allowed motion coherence manipulations to drive performance from chance to near perfect under all stimulus conditions.

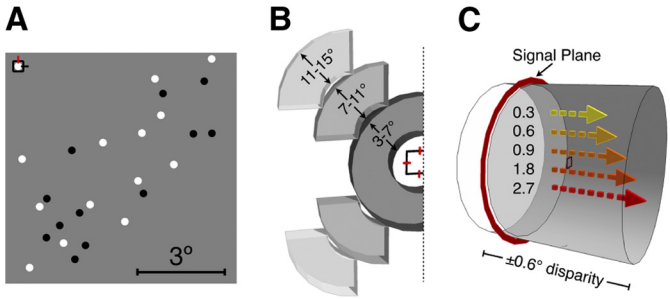

FIG. 2. Schematic of stimulus and manipulations. *A*: scale version of the stimulus as presented to the right eye. For clarity, this shows only the *bottom right* quadrant of the monocular stimulus. The fixation point and nonius lines are located in the *top lefthand* corner, with bright and dark stimulus dots scattered across an annular region 3–7° eccentric. Under all conditions the gray background extended across the entire monitor. By design, a single frame from one monocular image was identical (statistically) across all 3 motion cue stimuli. *B*: depiction of stimulus eccentricities. At the smallest eccentricity, signal and noise dots were restricted to an annular stimulus volume 3–7° from fixation. The smallest eccentricity was divided into 4 equal area quadrants (only the left 2 are shown, but the full display was left–right symmetric) that were displaced further outward for the other 2 eccentricity conditions, yielding eccentricities of 3–7°, 7–11°, and 11–15°. *C*: oblique depiction of the cyclopean 3D percept and speeds. A plane of signal dots moved through a cloud of noise dots (signal plane outlined in red for clarity; individual dots that actually constituted the plane not shown) and observers performed a 3D direction of motion discrimination (toward vs. away). The signal plane moved at one of 5 different speeds (colored arrows, in °/s·eye), corresponding to motions through depth, ranging from about 8 to about 72 cm/s (given our viewing distance of 70 cm). Direction discrimination sensitivity was measured at each of the 5 speeds (*C*) and 3 eccentricities (*B*), for each of the 3 motion cue types (see Fig. 3).

Observers fixated a small central square (0.5°) with horizontal (black) and vertical (red) nonius lines. A single dot (bright, 0.25° diameter, 0 arcmin disparity) was placed in the fixation square to provide subjects with an object of fixation and to prevent fixation drift toward endpoints of the fixation square or nonius lines. To further aid in proper binocular alignment, four stationary dots (dark, 0.5° diameter, 10.6° eccentric, 0 arcmin disparity) were located beyond the stimulus on horizontal and vertical axes of each monocular half-image. We used a sparse set of reference dots to limit extraneous relative disparity cues at the outer edges of the display (Andrews et al. 2001) while still providing eccentric visual anchor points.

Manipulations of eccentricity and speed

To examine how 3D motion sensitivity varies across the visual field, stimuli were presented within three different eccentricity ranges: 3–7, 7–11, and 11–15° from fixation (Fig. 2*B*). The "Near" eccentricity stimulus consisted of a continuous annular region spanning 3–7° from fixation. From this annulus, four 90° annular segments were then shifted outward in oblique directions (45, 135, 225, and 315°) to "Middle" and "Far" eccentricities of 7–11° and 11–15°, respectively. Thus the number and density of signal dots were held constant across the eccentricity conditions. Stimulus disparities were constrained to a volume spanning ±0.6° of disparity (i.e., along the *z*-axis) from the plane of fixation. At our 70-cm viewing distance, this corresponded to a total (front to back) simulated depth interval of 16 cm. This *z*-axis depth and thus the overall stimulus volume remained constant across all conditions.

To examine how 3D motion sensitivity varies with stimulus speed, stimuli were presented at five different speeds (where we define "speed" as the monocular angular speed in each eye): 0.3, 0.6, 0.9, 1.8, and 2.7°/s (Fig. 2*C*). Because we describe speed in degrees per second per eye (°/s·eye) and the monocular velocities were always opposite in the two eyes, one can simply multiply the monocular speeds times the number of eyes (two in our case) to calculate the equivalent disparity change in °/s.

Across all speeds, the total stimulus excursion through depth in a trial was always one full cycle through the stimulus volume (with a single "wrap" occurring on all trials, except those few in which the signal dots happened to begin at the very front or back of the volume). Stimulus presentations containing exactly one full cycle with a single depth wrap were chosen so that neither average depth (or disparity) over a trial, nor instantaneous depth (or disparity) at any point in the trial (e.g., starting or ending), could be used to perform the task. Given this one-cycle constraint, the resulting stimulus durations ranged from 2 s at the slowest speed to just over 0.2 s at the fastest speed (corresponding to 120 and 13 video frames, respectively). The decision to fix the total depth traveled (and not the overall duration of motion) was supported by three factors. First, our main inferences are based on comparisons of sensitivity across *FULL*, *CD*, and *IOVD* conditions, which effectively balances duration across the comparisons of interest. Second, given that we observed peak sensitivity in the main experiment at rather fast speeds (and thus at short durations), we are confident that shorter durations per se did not strongly impair performance. Third, exploratory manipulation of duration at the medium and high speeds revealed only a very small effect of stimulus duration that, in any event, was balanced across motion cue conditions in the main experiment.

Motion cue conditions: FULL, IOVD, and CD

Three motion cue stimuli were used: *FULL*, *IOVD*, and *CD*. All three stimulus types contained a single plane of signal dots moving toward or away from the observer through depth, in the presence of noise dots (described further in the following text). Figure 3 schematizes the three motion cue stimulus types.

The *FULL* stimulus consisted of a moving random dot stereogram in which binocularly paired signal dots moved in opposite directions in the two eyes. The signal dots thus contained both the IOVD and CD cues to 3D motion. Signal dots moved at constant monocular speeds ranging from 0.3 to 2.7°/s, corresponding to 3D motion speeds of about 8 to about 72 cm/s at our 70-cm viewing distance. Perceptually, the *FULL* stimulus resembled a fixed set of dots, not unlike a group of flying insects in a frontoparallel plane, moving directly toward or away from the observer in synchrony. All dot pairs (signal and noise) were binocularly correlated (i.e., were of the same contrast polarity across the eyes); noise dots are described in detail later and followed identical motion patterns across all three conditions.

The *IOVD* stimulus was identical to the *FULL* stimulus, except that all of the dot pairs were binocularly anticorrelated: each dark dot in one eye was paired with a corresponding bright dot in the other eye. Anticorrelation has been shown to disrupt static disparity mechanisms (Cogan et al. 1995; Cumming et al. 1998; Neri et al. 1999), while maintaining monocular velocity information (Harris and Rushton 2003) and thus retaining IOVDs in the presence of greatly degraded disparity-based signals. In addition, our group has previously used sparse, anticorrelated dot displays to isolate the contribution of the IOVD cue (Rokers et al. 2008, 2009). Perceptually, the *IOVD* stimulus is phenomenologically rather interesting (although this is not the direct subject of the current study). Because static disparity information is greatly compromised, one generally has the sensation of "something" moving toward or away from the eyes, with neither a firm sense of a distinct plane of dots present in space nor a sense of the position-in-depth of these moving elements.

The *CD* stimulus was identical to the *FULL* stimulus, except that the signal dots were randomly replotted in new *x*–*y* positions on the signal plane on each screen refresh (i.e., at 60 Hz). This replotting removed coherent monocular velocity information, while preserving steadily changing disparity information (Braddick 1974; Cumming and Parker 1994; Julesz 1971). For the *CD* stimulus, the rate of disparity change matched that of the *FULL* and *IOVD* stimuli. Per-

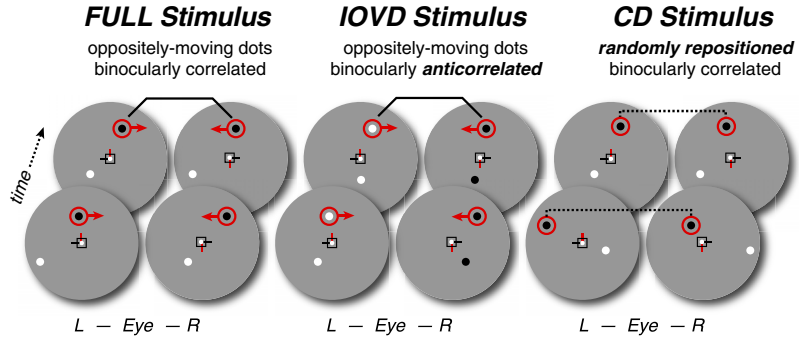

FIG. 3. Motion cue stimulus conditions. Depiction of representative signal dots from 2 example frames from each of the 3 stimulus conditions (from *left* to *right*: *FULL*, *IOVD*, *CD*). The half images in each set can be free-fused (*L*, left eye view; *R*, right eye view). In the *FULL* stimulus, corresponding dots moved in opposite directions in the 2 eyes. Such a stimulus contains both changing disparities (the *CD* cue) and interocular velocity differences (the *IOVD* cue). Red circles and arrows were not present in the actual stimulus, of course, but depict the respective motions of left and right eye's views of a single signal dot. Also note that actual dot densities were much higher (see Fig. 2*A* and METHODS): many similar signal dots specified a plane moving toward or away through depth. In the *IOVD* stimulus, corresponding dots also moved in opposite directions (just as in the *FULL* stimulus), but the dots were binocularly anticorrelated: a black dot in one eye was paired with a white dot in the other. This greatly reduced the contribution of the disparity-based *CD* cue, but the *IOVD* signal was preserved. In the *CD* stimulus, signal dots were randomly repositioned every frame, but their disparities (dotted brackets) still specified a signal plane moving toward or away through depth. The one-frame lifetimes of the dots removed any coherent monocular motions and thus eliminated the *IOVD* cue, while preserving the *CD* signal.

ceptually, the *CD* stimulus resembles a plane of TV snow moving through depth toward or away from the observer.

Manipulation of 3D motion coherence

The 3D motion coherence, defined as the ratio of signal dots to noise dots, was randomly varied on a trial-by-trial basis according to the method of constant stimuli. We determined direction-discrimination thresholds in units of motion coherence from the resulting psychometric functions.

At the beginning of each trial, the number of signal dots (as determined by the coherence level pseudorandomly drawn for that trial) was selected (out of the 80 total dots). The remainder were designated as noise dots. The signal dots were randomly positioned on a single frontoparallel plane moving toward or away from the observer. This signal plane began at a random position in depth and moved throughout the entire depth range (wrapping when necessary), ending in the same position in depth as it began. On wrapping, each signal dot was assigned a new random x–y position in addition to moving to the opposite end of the volume on the z-axis. For a given speed, this implied that the signal dots followed a uniform distribution of lifetimes between one frame and the number of frames in a trial at that speed (i.e., 120 frames at the slowest speed and 13 frames at the fastest speed). For any single trial, there were thus two signal dot lifetimes, one prewrap and one postwrap, which summed to the total number of frames in that trial.

We designed our noise dots to satisfy multiple, somewhat competing demands: *1*) remaining constant (statistically) across all conditions (cue type × speed × eccentricity); *2*) being capable of effectively masking the motion through depth of the signal plane across all conditions (and thus allowing us to measure psychometric functions spanning the full range of possible performance across all conditions); and *3*) effectively matching the spatiotemporal properties of the signal dots per se across all conditions—that is, we did not want the signal dots themselves to "pop out" in any condition due to either flashing on for one frame (*CD* condition) or persisting for multiple frames that varied with speed (*IOVD* and *FULL* conditions).

To satisfy these constraints, we used variable-lifetime noise dots that approximated random walks through depth. Their instantaneous (frame-to-frame) velocity was variable along the z-axis, but was constrained to be less than or equal to the signal dot velocity through depth (their x–y positions were fixed throughout each lifetime). Each noise dot was assigned a random lifetime ranging from one to 12 frames (16.7 to 200 ms) from an inverse-squared distribution. Specifically, the probability of a noise dot having a given lifetime L (in frames) was proportional to $1/L^2$, where $L = 1, 2, \ldots, 12$. At the expiration of a noise dot's lifetime, it was randomly repositioned within the stimulus volume and assigned a new lifetime from this distribution. [Our noise dots can therefore be considered a hybrid of the random-position and random-walk same-selection dot noise described in Scase et al. (1996).] At any given time, then, the noise consisted of a mixture of transient and persistent dots, like the *CD* signal dots on the one hand and the *IOVD* and *FULL* signal dots on the other, but with the distribution favoring the presence of short lifetime dots.

The distribution of noise dots included a higher proportion of shorter lifetimes because we reasoned that transient (flashing) elements are better at masking persistent elements than vice versa. Noise composed of mostly transient elements would be expected to mask both transient and persistent signals (which is important, given that our *CD* condition contained transient signal due to the single-frame lifetimes of the signal dots and our *FULL* and *IOVD* conditions contained more persistent signal due to the longer signal dot lifetimes). This argument can also be appreciated in the Fourier domain: transient noise elements will have broadband power in the temporal frequency domain and thus would cover the spectral range of signal across all conditions; persistent noise elements would be better localized in the temporal frequency domain and thus would not so broadly span the spectral range of signals of interest. Finally, pilot observations confirmed that noise from an inverse-squared distribution yielded good subjective degradation of the signal plane's direction of motion at high noise levels, provided good masking of the dots themselves across conditions (i.e., none of the signal dots popped out in any condition), and drove performance from an upper asymptote to chance levels for all motion cue types. We emphasize that these decisions allowed us to use noise dots that had the same distribution of motions and were subjected to the same manipulation of coherence (and thus the same sensitivity metric) across all conditions—a crucial component that enabled direct comparison of sensitivities across cue conditions.

Experimental design

We measured the observers' ability to discriminate the direction of motion through depth (toward or away) across a range of 3D motion coherence levels (0, 3, 6, 12, 24, and 50% coherence) using the method of constant stimuli. We used a fully crossed design containing all combinations of motion cue type (*FULL*, *CD*, *IOVD*), eccentricity

(3–7, 7–11, and 11–15°), and speed (0.3, 0.6, 0.9, 1.8, and 2.7°/s·eye). Within each run, we measured percentage correct as a function of motion coherence for a single combination of these factors (resulting in a single estimate of the psychometric function).

Motion coherence was pseudorandomized across trials within a run. Each run consisted of 40 trials per coherence level, resulting in 240 trials total. The order of runs was randomized. Each observer completed five runs of the 0.6, 0.9, and 2.7°/s·eye speeds for each motion cue/eccentricity combination, and three runs for each of the 0.3 and 1.8°/s·eye speeds. This resulted in either 720 or 1,200 trials per observer per condition and just under 45.4 kilotrials per observer for the main experiment. Two control experiments addressing position-in-depth and 2D motion discrimination (see DISCUSSION) contributed an additional approximately 20.2 kilotrials across the same three observers.

Apparatus and display

To investigate 3D motion perception at large eccentricity with high temporal accuracy, stimuli were presented on a calibrated 42-in. liquid crystal display (LCD) monitor (Sharp LC-42D64U; 60-Hz progressive scan 1,920 × 1,080 pixel resolution) viewed through a mirror stereoscope with a concomitantly large field of view. The monitor was driven by a Mac Pro computer and an NVIDIA GeForce 8800 GT video card.

Luminance calibrations were done at 10 locations across the display using an OptiCal photometer (Cambridge Research Systems). We verified that gamma correction tables for each location were the same across the entire luminance range, allowing all stimuli to be accurately presented using a single linearizing gamma correction table. All 10 curves were nearly identical within a scale factor, demonstrating a high degree of spatial luminance homogeneity, nearly perfect contrast homogeneity, and the ability to implement good luminance linearization with this LCD monitor.

We achieved spatial luminance homogeneity by making internal display adjustments. Specifically, the duty cycle of the LCD backlight was maximized by setting the "backlight" adjustment to the maximum level, while setting the "brightness" adjustment to the minimum level to maintain a comfortable luminance range. This provided the most homogeneous display luminance, leaving at most a 10% residual luminance variation that was almost entirely constrained to the extreme edges of the display (where stimuli were not presented).

Display timing was verified using a fast photocell (Model 10AP; UDT Sensors, Hawthorne, CA) and an oscilloscope. We used a splitter-cable so that we could measure the VBL signal directly while simultaneously measuring the instantaneous luminance on the monitor. Pixel updates were constant at 60 Hz and at a fixed phase relative to the VBL signal generated by the video card. The white-to-black transition was marginally faster than the black-to-white, with the latter showing slight exponential characteristics. Nonetheless, the display easily followed repeating black-white and black-gray-white-gray cycles on a frame-by-frame basis at 60 Hz. Although the display was slow by modern cathode ray tube standards, it provided reliable timing of display updates, as well as luminance output that was easily linearized. Furthermore, all in-monitor enhancement modes (e.g., motion enhancement, dynamic contrast adjustment, etc.) were disabled because they could yield undesirable display artifacts. In short, our measurements suggested that our particular LCD was appropriate for use in our experiments; it remains to be seen whether similar results can be attained by similar adjustment and calibration using other LCDs.

Monocular half-images were presented separately on the left and right halves of the display, with a septum and various baffles positioned to ensure that each half-image was visible only to the corresponding eye. Viewed through the 70-cm optical path length of the stereoscope, each monocular half-image subtended 30° of visual angle. This display arrangement was selected over traditional dual-display stereo or shutter goggle apparatus because it provided both perfect temporal synchronization between the two eyes and complete isolation of the monocular half-images. All stimuli were generated using the Psychophysics Toolbox (Brainard 1997) and MATLAB (v. 2007a; The MathWorks, Natick, MA).

Data analysis

For each condition (motion cue type × eccentricity × speed), we combined data across multiple runs for each subject and fit a logistic psychometric function using the psignifit toolbox version 2.5.6 for Matlab (http://bootstrap-software.org/psignifit/). Threshold was defined as the 3D motion coherence yielding 84% accuracy. We bootstrapped confidence intervals (equivalent to ±1SE) about these thresholds by resampling (with replacement) the binomial responses from each subject to create 500 repetitions of the experiment, fitting a psychometric function to each resampled experiment, and identifying the central 68% of the values. In instances where observers were unable to discriminate 3D motion direction we assigned a threshold coherence of 100% (pinning the thresholds at the maximum physically realizable level was preferable to simply discarding those data, but our conclusions do not change if these are instead omitted). Across a total of 135 sensitivity estimates (3 observers, 5 speeds, 3 eccentricities, 3 cues) this occurred only seven times and was isolated to high-speed *CD* stimulus conditions.[3]

We applied a similar resampling approach when fitting the eccentricity and speed-tuning curves (Figs. 4 and 5). We plotted the median fit parameters (after checking that the median values were very similar to the means) because the medians had the advantage of being robust to the occasional extreme values that can arise in a small number of fits across the very large number of resampled data sets.

RESULTS

Recall that, in all conditions, observers simply judged whether a plane of signal dots was moving toward or away from them. On each trial, stimuli were presented at one of six different motion coherence levels (0, 3, 6, 12, 24, and 50% coherence). Sensitivity (inverse 3D motion coherence threshold) was then estimated for each combination of eccentricity (Near, Middle, and Far), speed (0.3, 0.6, 0.9, 1.8, and 2.7°/s·eye), and motion cue type (*FULL*, *CD*, and *IOVD*).

In each of the following sections, we first establish a baseline for 3D motion discrimination by describing the performance in the *FULL* cue condition, which contained both disparity- and velocity-based 3D motion cues (CD + IOVD). We then compare the results to each isolated cue condition (*CD*, *IOVD*). To explore how sensitivity varied across the entire eccentricity–speed space, we address the results from three perspectives in the following three sections: the effects of eccentricity at different speeds, the effects of speed at different eccentricities, and finally, the full spatiotemporal (speed × eccentricity) sensitivity surface. (Unless otherwise noted, data points in the following figures represent mean sensitivity across all three observers.)

Effects of eccentricity at different speeds

Here, we first describe the data as functions of eccentricity measured at different speeds. Figure 4 (*left*) shows the eccen-

[3] Specifically, observer ACH was unable to discriminate *CD* stimulus direction at the three highest speeds in the farthest eccentricity conditions (11° eccent.; 0., 1., and 2. °/s·eye) and at the highest speed in the middle eccentricity condition (7° eccent.; 2. °/s·eye). Observer LKC was unable to discriminate *CD* stimulus direction at any eccentricity at the highest speed (3, 7, 11° eccent.; 2. °/s·eye).

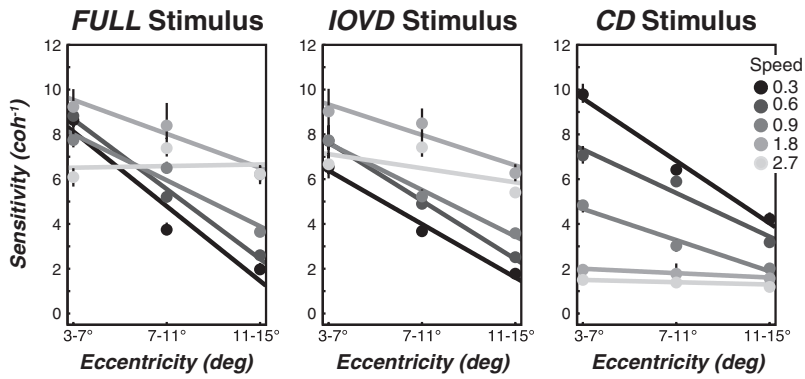

FIG. 4. 3D motion direction–discrimination sensitivity as function of eccentricity (and speed). Direction-discrimination sensitivity (*y*-axis) as a function of eccentricity (*x*-axis), with speed as the grouping parameter (lighter shades of gray corresponding to faster speeds). Error bars represent 68% bootstrapped confidence intervals (i.e., SEs). For both the *FULL* (*left*) and *IOVD* (*middle*) conditions, sensitivity decreased with increasing eccentricity. Moreover, sensitivity generally increased with increasing speed for these 2 conditions, particularly at higher eccentricities. Only for the very fastest speed did sensitivity begin to decrease (this effect was most pronounced at the smallest eccentricity). The pattern in the *CD* condition (*right*) was strikingly different: sensitivity did decrease with increasing eccentricity and more so for slowest speeds, but the overall order of the curves was reversed, with low speeds yielding much higher sensitivities than high speeds.

tricity effect on *FULL* stimulus sensitivity across the range of 3D motion speeds. Increases in stimulus eccentricity caused a decrease in direction-discrimination sensitivity in a speed-dependent manner. The strength of this effect can be determined from the slope of linear fits at each stimulus speed. Sensitivity to slower 3D motion (darker curves and symbols) was strongly diminished by increasing eccentricity (slope of -0.83 coh^{-1}·deg^{-1} at slowest speed, 0.3°/s·eye), whereas sensitivity for faster 3D motions (lighter gray curves and symbols) was not strongly affected by eccentricity (slope of 0.02 coh^{-1}·deg^{-1} at fastest speed, 2.7°/s·eye). The eccentricity effect was smaller at the highest speed primarily due to a large improvement in sensitivity at the Far eccentricity; sensitivity at the Near eccentricity did not change as much. In summary, eccentricity reduced direction-discrimination sensitivity in the *FULL* condition, but did so strongly for slower speeds and less so for faster speeds.

Sensitivity to the *IOVD* stimulus (Fig. 4, *middle*) showed a similar pattern of eccentricity dependence as the *FULL* stimulus. Sensitivity to *IOVD* motion was strongly affected by eccentricity at slower speeds (slope of -0.60 coh^{-1}·deg^{-1} at the slowest speed, 0.3°/s·eye) and was less affected by eccentricity at higher speeds (slope of -0.16 coh^{-1}·deg^{-1} at the fastest speed, 2.7°/s·eye). As with the *FULL* stimulus, the change in eccentricity function across speeds was more the result of changes in sensitivity at Far eccentricity than at Near eccentricity. So, just as for the *FULL* condition, eccentricity effects for the *IOVD* condition were larger at slower speeds and smaller at higher speeds.

Sensitivity to the *CD* stimulus (Fig. 4, *right*) followed a pattern that was strikingly different from that seen from the *FULL* and *IOVD* stimuli. Larger eccentricity did yield poorer performance in general and eccentricity effects were steepest at the slower speeds. At the higher speeds, however, performance was very poor regardless of eccentricity. At the highest speed, in fact, only one observer was able to reliably perform above chance. In other words, the lack of an eccentricity effect at high speeds is probably best thought of not as a uniform sensitivity across eccentricities per se, but rather as an overall lack of sensitivity of the CD system to stimuli moving rapidly in depth.

In summary, the effects of eccentricity on *FULL* and *IOVD* sensitivity were quite similar and showed similar dependencies on speed. In contrast, *CD* sensitivity followed a very different pattern of interactions between eccentricity and speed. The nature of this interaction becomes more clear in the next section.

Effects of speed at different eccentricities

It is perhaps more illuminating to consider the same sensitivity data as speed-tuning curves measured at different eccentricities, as shown in Fig. 5 (note the log speed axis). For the *FULL* stimulus (Fig. 5, *left*) similar band-pass speed-tuning functions were evident at all stimulus eccentricities, peaking near the higher speeds measured. At Near eccentricity, sensitivity fell off sharply for speeds faster than 1.8°/s·eye. Because of the band-pass appearance, we fit the data with Gaussian functions. The peak of the fitted Gaussian for the Near data were at 1.09°/s·eye, with a full width at half the maximum (FWHM) height of 3.92°/s·eye. At Middle and Far eccentricities, peak sensitivity shifted toward even higher stimulus speeds (Middle,1.94°/s·eye; Far, 2.27°/s·eye). The stronger effects of eccentricity at low speeds had the effect of narrowing the band-pass speed tuning at Middle and Far eccentricities (FWHM, Middle, 3.23°/s·eye; Far, 3.12°/s·eye).

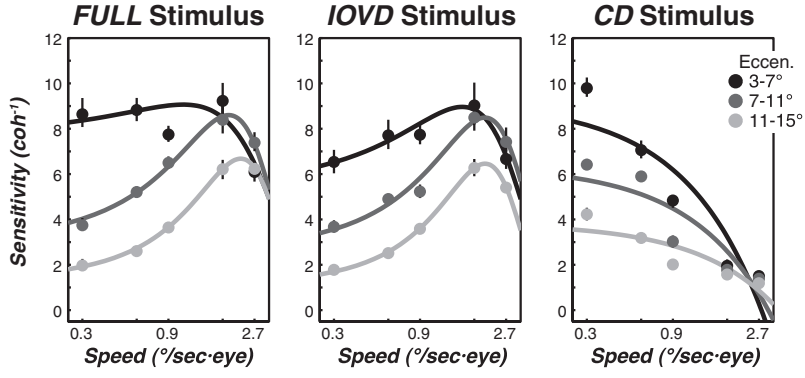

FIG. 5. 3D motion direction–discrimination sensitivity as function of speed (and eccentricity). Direction-discrimination sensitivity (*y*-axis) as a function of speed (*x*-axis), with eccentricity as the grouping parameter (lighter shades of gray corresponding to larger eccentricities). The speed axis is logarithmic, error bars represent 68% bootstrapped confidence intervals. For both the *FULL* (*left*) and *IOVD* (*middle*) conditions, sensitivity shows distinct band-pass tuning, with peak sensitivity occurring just before the highest speeds tested. In contrast, sensitivity in the *CD* condition (*right*) exhibited clear low-pass tuning, with maximal sensitivity for the speed closest to stationary. For all conditions, sensitivity generally increased with decreasing eccentricity (dark curves above light curves). Although at faster speeds sensitivity for *FULL* and *IOVD* conditions was generally higher than that for the *CD* condition, note also that at the lowest speeds, sensitivity for the *CD* condition actually exceeded that of the *FULL* cue condition.

The pattern of *IOVD* sensitivity (Fig. 5, *middle*) was again strikingly similar to the *FULL* stimulus. Sensitivity was band-pass for speed with a peak near the higher speeds. This band-pass tuning was evident at all eccentricities and *IOVD* peak sensitivity also followed a pattern similar to that for the *FULL* stimulus. Peak speeds were 1.54, 2.06, and 2.06°/s·eye for Near, Middle, and Far eccentricities, respectively, and likewise became more sharply speed-tuned with increasing eccentricity (FWHMs were 3.49, 3.23, and 2.91°/s·eye, respectively). The similarity between the *FULL* and *IOVD* patterns of speed tuning is further supported by a point-by-point comparison of the two tuning functions, revealing that 12 of the 15 points fall within 68% (±1SE) confidence intervals of one another.

The *CD* condition demonstrated an altogether different pattern of sensitivity from those seen in the *FULL* or *IOVD* conditions (Fig. 5, *right*). All of the speed-tuning curves were clearly low-pass, falling off precipitously with increasing speed (i.e., only one observer was able to discriminate the highest speed *CD* stimuli at accuracies above chance). In fact, the difference in the tuning curves was pronounced enough that we could not fit the *CD* data satisfactorily with Gaussians given reasonable parameter values and we therefore fit them with straight lines. Fitted linear slopes were all strongly negative (in units of sensitivity, $coh^{-1}\cdot deg^{-1}\cdot s^{-1}$: Near, −3.28; Middle, −2.09; Far, −1.10). As with the eccentricity effects in the previous section, the slopes of the speed effects on the *CD* stimulus became less steep at far eccentricities simply because accuracy levels fell toward chance.

In summary, the analysis of speed tuning reveals that IOVD-based performance closely mirrored that of full-cue performance. *FULL* and *IOVD* speed tuning was band-pass, with a peak at relatively brisk 3D motion speeds. In contrast, CD-based performance exhibited dramatically different speed tuning that cannot account for most of the full-cue sensitivity. Instead, *CD* speed tuning was low-pass and fell off steeply near the speeds at which the *IOVD* and *FULL* conditions revealed maximal sensitivity. Although the stimuli and tasks were different, these speed-tuning results are qualitatively consistent with the temporal frequency-tuning results of Shioiri et al. (2008).

Speed by eccentricity (S × E) sensitivity surface

The preceding sections show that *IOVD* sensitivity is very similar to *FULL* sensitivity, and that *CD* sensitivity follows a rather different pattern, regardless of whether the data are viewed as slices of constant speed or constant eccentricity. The overall shape of the data for the three conditions can be appreciated more thoroughly in spatiotemporal sensitivity surface contours that span both eccentricity and speed (Fig. 6). The *top row* depicts the sensitivity surface for each motion cue condition: stimulus eccentricity by speed (S × E) on the *x*- and *y*-axes, respectively, and direction-discrimination sensitivity on the *z*-axis (height). The surface sensitivities are also projected down to contour maps on the $z = 0$ plane. Band-pass speed sensitivity can be seen in both *FULL* and *IOVD* conditions, as can the weaker eccentricity effects closer to the best speed. In contrast, the *CD* condition shows a distinct pattern of roughly linear sensitivity falloff as speed and eccentricity increase.

The bottom row of surface-contour plots (Fig. 6) show the *differential* sensitivity surfaces generated by subtracting the spatiotemporal sensitivity surfaces of each motion cue. Positive values are shown in the same warm color map as the original sensitivity surfaces, whereas negative values are shown in cool colors extending below the contour map. The left two panels of the bottom row of surface-contour plots show differential sensitivity surfaces generated by subtracting each isolated cue surface from the *FULL* stimulus surface (i.e.,

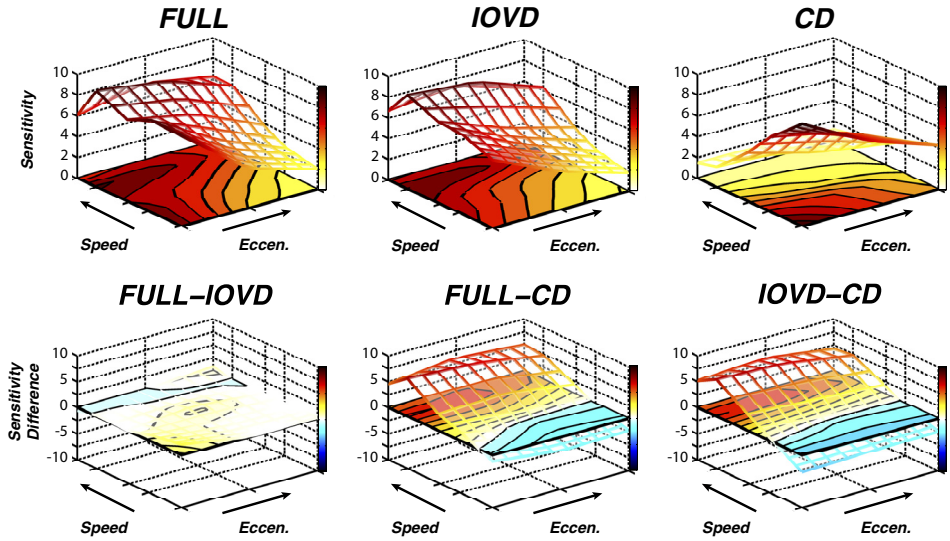

FIG. 6. 3D motion direction–discrimination sensitivity as a function of both speed and eccentricity. *Top row*: sensitivity as a function of both speed and eccentricity for the 3 cue conditions. Each sensitivity surface represents combined subject data from 45,360 trials. Height of mesh (*z*-axis) indicates sensitivity, as a function of speed and eccentricity (*x* and *y* axes). Colored floor is a contour plot depicting the same sensitivity information. The *FULL* and *IOVD* surfaces are quite similar, whereas the *CD* surface is distinctly different (so much so that, from this perspective, the view is of the bottom of the mesh surface). *Bottom row*: differential sensitivity surfaces highlighting the similarity, or lack thereof, between the 3 conditions ($z = 0$ plane has been raised to allow for negative values). The *FULL–IOVD* surface is nearly flat, indicating substantial similarity. In contrast, the other 2 surfaces (*FULL–CD*, *IOVD–CD*) show a systematic pattern of differences. At the slowest speed tested, *CD* sensitivity was higher than *IOVD* sensitivity and higher than the *FULL* sensitivity as well (cool colored mesh and surface).

TABLE 1. *P values on 3D motion sensitivity difference surfaces*

Speed	Near	Middle	Far
	FULL–IOVD		
0.3°/s·eye	0.004*	0.416	0.278
0.6°/s·eye	0.090	0.200	0.322
0.9°/s·eye	0.476	0.002*	0.416
1.8°/s·eye	0.436	0.462	0.462
2.7°/s·eye	0.162	0.460	0.034
	FULL–CD		
0.3°/s·eye	0.066	0.000*	0.000*
0.6°/s·eye	0.012*	0.020*	0.006*
0.9°/s·eye	0.000*	0.000*	0.000*
1.8°/s·eye	0.000*	0.000*	0.000*
2.7°/s·eye	0.000*	0.000*	0.000*
	IOVD–CD		
0.3°/s·eye	0.000*	0.000*	0.000*
0.6°/s·eye	0.198	0.004*	0.002*
0.9°/s·eye	0.000*	0.000*	0.000*
1.8°/s·eye	0.000*	0.000*	0.000*
2.7°/s·eye	0.000*	0.000*	0.000*

*$P < 0.05$.

FULL–IOVD, *FULL–CD*). The surface goes positive (above the contour map) where sensitivity is better in the *FULL* stimulus and the surface goes negative (below the contour map) where sensitivity is better in an isolated cue condition (IOVD or CD). Bootstrapped *P* values for the difference surfaces are shown in Table 1.

The *FULL–IOVD* surface shown in the bottom left panel is nearly flat, indicating that the sensitivities are nearly identical at each combination of speed and eccentricity tested. In fact, only 2 of the 15 points in the *FULL–IOVD* surface are significantly different from zero.

The *FULL–CD* surface shown in the bottom middle panel, however, is distinctly not flat. For faster speeds, observers are much more sensitive to the *FULL* stimulus than the *CD* stimulus, indicating that the (lack of) CD sensitivity does not limit the observers' performance. For the slowest speeds, on the other hand, observers actually performed better in the *CD* condition than they did in the *FULL* condition, indicating that: *1*) observers were unable to fully exploit the changing disparity information when interocular velocity differences were also present and/or *2*) there was richer changing-disparity information present in the *CD* stimulus than in the *FULL* stimulus (perhaps due to the faster temporal refresh rate of the signal dots in the *CD* condition). Regardless of which possibility is at work (both could be), this superiority of the *CD* condition for slow speeds demonstrates that the larger-scale dissimilarity between the *FULL* and *CD* conditions is not simply because the *CD* stimulus did not contain a strong signal.

The bottom right surface-contour plot shows the differential sensitivity surface generated by subtracting the CD sensitivity surface from the IOVD sensitivity surface (*IOVD* − *CD*). Obviously, this difference surface closely resembles the *FULL–CD* surface and it can also be thought of as a visualization of the relative utility of the two (isolated) cues in our experimental conditions.

The ability of each isolated cue to predict the *FULL* sensitivity is shown in Fig. 7. Individual observer sensitivities for each isolated cue condition (*y*-axis) are plotted as function of *FULL* stimulus sensitivity (*x*-axis). Each data point, in other words, shows a pair of thresholds for a particular combination of observer, speed, and eccentricity. The left scatterplot shows a high level of correlation between the *IOVD* and *FULL* stimulus sensitivities ($r^2 = 0.75$). This strong correlation on an individual subject level suggests that *FULL* sensitivity can be accurately predicted simply by measuring an individual's corresponding *IOVD* sensitivity in isolation. However, this relationship does not hold for the right scatterplot of *CD* versus *FULL* sensitivities ($r^2 = 0.05$). Thus knowing an individual's *CD* sensitivity does not provide much information to predict how well the observer will be able to discriminate the direction of realistic (full-cue) motions through depth. Interestingly, Watanabe et al. (2008) found a very similar pattern of results when comparing their novel clinical test for motion through depth with a standard static stereo test (Titmus).

DISCUSSION

Our experiments revealed distinctly different patterns of sensitivity to the changing disparity (CD) and interocular velocity difference (IOVD) cues for 3D motion direction discrimination. Sensitivity to the CD cue was highest at the shortest eccentricities and the slowest speeds. Increasing either speed or eccentricity had strong and independently deleterious effects on *CD* sensitivity. Sensitivity to the IOVD cue, on the other hand, was lowest at the nearest eccentricities and the slowest speeds. Increasing speed led to greater *IOVD* sensitivity and mitigated the effects of eccentricity. Overall, the pattern of *IOVD* sensitivity was nearly identical to the pattern of *FULL* sensitivity—sensitivity for stimuli containing both the CD and the IOVD cues—across the entire eccentricity–speed space. In contrast, the pattern of *CD* sensitivity across the eccentricity–speed space was markedly different from the *FULL* pattern. Although these patterns of relative sensitivity were not as straightforwardly dependent on speed and eccentricity as we initially hypothesized, they did reveal a surprisingly close correspondence between *IOVD* and *FULL* sensitivity across the majority of the wide spatiotemporal range we investigated. We therefore conclude that, at least outside the fovea, the human visual system can rely primarily on interocular velocity

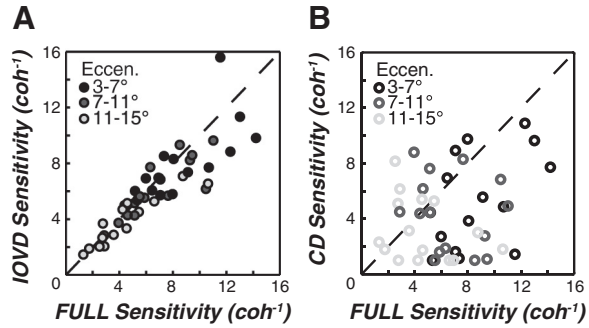

FIG. 7. Comparison of *IOVD* sensitivity and *CD* sensitivity to *FULL* sensitivity. Scatterplots show *IOVD* sensitivity (*A*) and *CD* sensitivity (*B*) plotted on the *y*-axis against corresponding *FULL* sensitivity (*x*-axis). Each data point corresponds to the sensitivity of an individual subject for a particular eccentricity/speed/motion cue condition. Lighter gray symbols represent farther eccentricities. The dashed line shows unity. *IOVD* sensitivity generally matched *FULL* sensitivity ($r^2 = 0.75$), whereas *CD* sensitivity was relatively unrelated ($r^2 = 0.05$), illustrating that *FULL* sensitivity is better predicted by *IOVD* sensitivity than by *CD* sensitivity.

differences, not changing disparities, to discriminate the direction of 3D motion.

Distinguishing the contributions of the CD and IOVD cues

The differential patterns of sensitivity across the eccentricity–speed space provide clear evidence for a dissociation of the CD and IOVD cues. The disparity-based cue functions best at slow speeds and nearer eccentricities, whereas the velocity-based cue exhibits band-pass sensitivity for higher speeds, with muted eccentricity effects. These distinct patterns of sensitivity suggest that the CD cue may be useful for slow-moving (para-)foveal 3D motions and that the IOVD cue may be more useful for faster and more peripheral 3D motions.

Our results also provide additional support to the notion that the IOVD cue can be experimentally isolated. We addressed the effectiveness of anticorrelation in isolating the IOVD cue by conducting two experimental controls: *1*) to determine whether useful position-in-depth information could be contributing to 3D motion sensitivities in the *IOVD* stimuli and *2*) to rule out the possibility that similarities in *FULL* and *IOVD* sensitivities could result from simple monocular motion sensitivities.

Unlike the CD cue, the IOVD cue cannot be perfectly isolated in principle. Although contrast anticorrelation is not a perfect form of isolation, we believe it is currently the most effective method of removing useful disparity information from a stimulus (and thus strongly biasing the stimuli in favor of IOVD mechanisms). There are two primary concerns that are often raised about these anticorrelated stimuli. The first is that, in an anticorrelated stimulus, there are many potential "false" matches of the same contrast polarity (e.g., a given white dot in one eye could conceivably be matched with any other white dot in the other eye's image, even though the experimenter had specified that the "corresponding" dot be of opposite contrast polarity). There are several reasons why it is unlikely that these potential unintended matches influenced the data in a meaningful way. First, given the dot density of our stimuli, any unintended matches would have a large disparity, usually both horizontal and vertical, and these would vary from match to match at any given time (thus a vertical vergence movement, for example, could not suddenly create a large number of plausible, predominantly horizontal disparities). Because the effective signal of a binocular element falls off with the overall disparity, regardless of how "effective signal" is determined, the majority of these matches would not be a very effective stimulus (Blakemore 1970; Cormack et al. 1993; Prince et al. 2002; Stevenson et al. 1992, 1994). Second, at threshold values of coherence, the vast majority of these potential matches for a given signal dot in one eye would be with a noise dot in the other eye. The match would thus result in an additional binocular noise dot (or at least a much noisier signal dot). If performance in the IOVD conditions were based on these spurious disparity signals, then it would be quite poor indeed. Rather, we find that the data from the *IOVD* conditions tracks that from the *FULL* conditions, despite the huge difference in the quality of the disparity signals. Even under the most general assumptions about the presence of an unintended CD signal in our IOVD stimulus, our data are inconsistent with this explanation.

The second potential problem with anticorrelated stimuli is that each dot contains two vertical (on average) edge segments of opposite contrast polarity, so it is conceivable that, for example, the left edge of a white dot could be paired with the right edge of the corresponding black dot. However, these matches would be between regions of different overall (signed) contrast and local mean luminance and it is known that unequal contrast between corresponding elements in the two eyes impairs stereopsis very dramatically—much more so than an overall contrast reduction (Cormack et al. 1991).

However unlikely, these concerns are valid in principle, so we addressed them by conducting a control experiment where observers performed coarse position-in-depth judgments (two-alternative, forced choice [2AFC] discrimination of the signal dots as near or far relative to the plane of fixation), while viewing stimuli moving at 0.9°/s·eye under each motion cue/eccentricity combination. The position-in-depth judgments were performed on stimuli nearly identical to those of the main experiment except that one eye's image was flipped horizontally, so that the motion was in the same direction in the two eyes. This created moving (frontoparallel) stimuli with a fixed, random disparity offset in each trial while still maintaining the same monocular motions as in the main experiment.

When observers were asked to discriminate whether this plane of dots was near or far relative to the zero-disparity plane of fixation, performance with the anticorrelated (*IOVD*) stimulus was so poor that we could not measure psychometric functions and report thresholds. We therefore did the following analysis: For each eccentricity and observer, we noted the 84% correct threshold 3D motion coherence for the *FULL* stimuli. We then measured position-in-depth performance for each observer and eccentricity at this coherence for each stimulus type. So if, for example, there was rich disparity information extracted from the anticorrelated stimulus (say, stemming from an early rectifying nonlinearity), then performance in the disparity-based position-in-depth task should be close to 84% correct. If, on the other hand, the anticorrelated stimulus does indeed greatly reduce the available disparity information, performance should be much poorer than 84% correct.

Figure 8*A* is a plot of the mean performance across subjects in the position-in-depth task for each cue type as a function of eccentricity and tested at the corresponding 3D motion threshold coherence. The subjects all behaved very similarly (error bars are ±1SE across the three subjects and are smaller than the symbols for four of the nine points). Two trends are clear. First, (static) depth judgments for the CD stimuli at the 3D motion coherence threshold are better than 84% correct, confirming the rich disparity signals present in these stimuli. Second, and importantly for our purposes, performance for all observers at all eccentricities was at or near chance for the *IOVD* stimuli, even though the same stimulus coherences supported 84% correct performance on the 3D motion task. This indicates that, whatever the potential disparity information is in the anticorrelated stimuli, observers were unable to use it to do basic depth discriminations.

The near-absolute failure to accurately judge position-in-depth on *IOVD* stimuli implies that any disparity signals arising from the anticorrelated elements were not perceptually accessible for the purposes of performing a simple near-versus-far task. These observations support the notion that direction discrimination of our *IOVD* stimulus in the main experiment

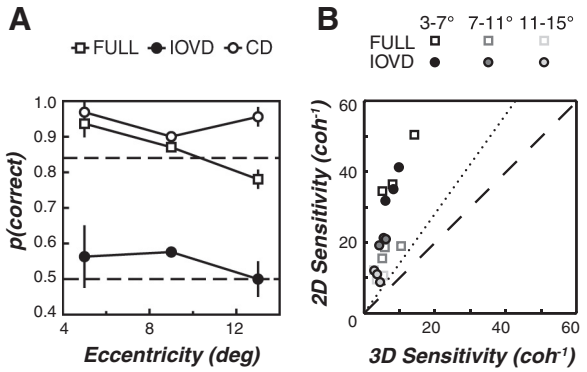

FIG. 8. Isolation of *IOVD* cue. *A*: position-in-depth performance (proportion correct for a near vs. far 2-alternative, forced choice [2AFC] discrimination) for the *CD* (open circles), *IOVD* (closed circles), and *FULL* stimuli (open squares). Each point represents the position-in-depth performance (averaged over 3 observers) as measured at the motion coherence corresponding to each observer's 3D motion direction-discrimination threshold. *CD* position-in-depth performance was much better than that of *IOVD* at all eccentricities (and even better than that for the *FULL* stimulus in one case). Crucially, *CD* performance was always better than 84% correct (top dashed line indicates the performance level for the 3D motion task at the coherences used), but *IOVD* performance was at or near chance (bottom dashed line). *B*: individual observer's 2D motion direction–discrimination sensitivity for the *FULL* (open squares) and *IOVD* (closed circles) stimuli as a function of the corresponding 3D motion direction–discrimination sensitivity. All of the points fall above the dashed line (unity), indicating the much greater sensitivity to 2D frontoparallel motion than to 3D motion. The dotted line (root-2 improvement 2D vs. 3D) suggests that the greater sensitivity to 2D motion cannot be explained by simple within-direction binocular summation.

was based on the interocular comparisons of velocities, with effectively no contribution of residual disparity signals that might have been used to compute an additional CD signal. This control experiment replicates and expands our previous dissociation of percepts of motion through depth from percepts of position-in-depth using similar anticorrelated stimuli (Rokers et al. 2008). Although it could be argued that the computations of static and dynamic disparity mechanisms may be distinct processes, we believe that the term "changing disparity" should (and has been) defined as a signal that takes conventional suprathreshold static disparity signals as its input. Thus if it can be demonstrated that a given stimulus configuration does not support depth judgments based on static disparities, then it cannot support 3D motion judgments based on changing disparities. This disparity hierarchy appears to hold in both classical and recent models of CD mechanisms (Cumming 1995; Peng and Shi 2010).

We ruled out another concern regarding the *IOVD* stimuli, which is that observers might have performed the direction-discrimination task on the basis of monocular direction discrimination instead of based on perceived 3D direction per se. If this were the case, the intrinsic monocular similarities of the *FULL* and *IOVD* stimuli could account for the similar sensitivities observed. Of course, this argument assumes that subjects were able to perform the task using concurrent utrocular identification and 2D direction discrimination under conditions of simultaneous stimulation in the two eyes (which is rather unlikely; see Ono and Barbeito 1985; Porac and Coren 1986) and also correctly mapping the monocular motion to the 3D direction in the absence of feedback. Regardless, we addressed this concern empirically, by performing an additional experiment in which we measured the observers' frontoparallel (2D) direction-discrimination sensitivity for *FULL* and *IOVD* stimuli, and compared them to their corresponding 3D motion sensitivities from the main experiment. This 2D direction-discrimination task was performed on identical stimuli as in the position-in-depth task (described earlier), except that observers were instructed to respond to the 2D direction of motion (leftward or rightward). The scatterplot of these data (Fig. 8*B*) shows that sensitivity for 2D direction discrimination was several times higher than equivalent 3D motion sensitivities across all eccentricity and motion cue conditions. This replicates stereomotion suppression (Tyler 1971) and supports a larger body of research that has shown that IOVD performance cannot be explained on the basis of monocular stimulation (e.g., Brooks and Stone 2006; Harris and Watamaniuk 1995; Rokers et al. 2008; Shioiri et al. 2000).

Although prior work has shown that the CD cue can be experimentally isolated and is sufficient to yield percepts of 3D motion (Cumming and Parker 1994; Gray and Regan 1996; Julesz 1971; Norcia and Tyler 1984), our results suggest that the IOVD cue can be similarly studied in near-isolation by using binocularly anticorrelated elements outside the fovea, moving at moderately fast speeds, at relatively sparse densities (more akin to displays traditionally used to study frontoparallel motion than those used to study stereopsis). Our results also suggest that the IOVD cue is not only sufficient to yield percepts of 3D motion, but is also relied on preferentially (relative to the CD cue) under many viewing conditions.

Effects of speed on the CD and IOVD mechanisms

The CD and IOVD mechanisms were affected very differently by manipulations of speed. *CD* sensitivity fell quickly with increased speed, exhibiting a low-pass sensitivity (or having a peak at or lower than the lowest speeds measured). *IOVD* sensitivity, on the other hand, had a clearly band-pass sensitivity peaking at a faster speed. *FULL* sensitivity also exhibited a band-pass speed tuning, one that was nearly identical to the *IOVD* pattern, but that contrasted sharply with that seen for the CD stimuli.

We described our stimulus motions in terms of retinal speed per eye (or, in the case of the *CD* stimulus, equivalent retinal speed per eye). For example, a speed of "1.8°/s·eye" corresponds to rightward (or leftward) monocular motion in one eye at 1.8°/s and leftward (or rightward) monocular motion in the other eye at 1.8°/s. Such a speed, although relatively slow when viewed monocularly, yields a percept of relatively fast motion through depth toward or away from the observer. This speed was closest to the peak of the *IOVD* and *FULL* speed-tuning curves. Likewise, at 0.3°/s·eye, the qualitative percept was of very slow displacement over time and observers reported that this condition did not yield a "direct" perception of motion through depth—rather, the phenomenology was of inferring motion from a change in position-in-depth over time. It is thus noteworthy that this speed yielded the highest *CD* sensitivity.

The effects of speed suggest that the perception of 3D motion in natural stimuli (which inherently contain both binocular cues) appears to be supported by the IOVD cue more than the CD cue. That said, the CD cue appears well-suited to carry information for very slow 3D motions. One possibility is that the CD mechanism is not fundamentally a motion mech-

anism, but rather one optimized for objects that are (nearly) stationary. The (isolated) CD signal can drive vergence eye movements, but these are relatively sluggish—generally $<1°$/s (Stevenson et al. 1994). We speculate that the CD mechanism may simply reflect the brain's attempt at inferring the pattern and rate of change of signals from well-characterized "static" disparity detectors. In contrast, the IOVD mechanism appears to be more similar to other (2D) motion mechanisms and is well-suited to quickly moving objects. The pattern of sensitivity we observed to the FULL cue displays further suggests that the human visual system is capable of relying on this IOVD mechanism. This is ecologically appropriate, given that sensitivity to objects moving quickly toward or away (even if they have not yet been fixated) is likely a major element in successful interaction with a dynamic 3D environment.

Eccentricity effects on the CD and IOVD mechanisms

The patterns of sensitivity to the CD and IOVD cues across a wide eccentricity range complement the observed effects of speed. Sensitivity to *FULL*, *CD*, and *IOVD* stimuli decreased at larger eccentricities. When considered in isolation, the manipulation of eccentricity was actually less effective at distinguishing between the CD and IOVD cues. One might have expected that *CD* sensitivity would be particularly affected by eccentricity because the processing of static disparities is known to be much better in the fovea (e.g., Blakemore 1970; Tyler 1975). However, displays that simulate reasonable 3D motions subtend a disparity range that is at least an order of magnitude greater than the stereoacuity threshold at the eccentricities tested (Westheimer and Truong 1988). Thus even the most eccentric stimuli (11–15°) still contained a range of disparities that could likely have supported *CD* sensitivity at higher eccentricities.

Instead, the effects of eccentricity are more informative when one considers them in conjunction with the manipulation of speed. *IOVD* sensitivity was relatively more robust to eccentricity for faster speeds of motion through depth. This improvement with speed is further consistent with the notion that our anticorrelated *IOVD* stimulus tapped a motion mechanism. For example, sensitivity to temporal frequency is, if anything, improved at far eccentricities (Rovamo and Raninen 1984; Wright 1987). Indeed, the eccentricity effects on *IOVD* sensitivity were lowest at fast speeds, perhaps because performance had achieved a maximal level. In contrast, eccentricity effects on *CD* sensitivity were lowest at fast speeds as well, but in this case, the reason was because performance was approaching chance (instead of peak performance) levels.

Taken together, the consideration of speed and eccentricity effects would suggest that the CD mechanism is capable of supporting 3D motion direction discrimination for slow (and particularly parafoveal) motions. Outside of this range, the IOVD mechanism appears much more capable of accounting for 3D direction discrimination when both cues are present. We interpret this as evidence for the relative primacy of the IOVD cue outside central vision. The visual system may exploit interocular velocity differences as a robust source of information for moderate- and fast-moving objects that one is not (yet) looking at. This suggests that classical motion detectors, typically studied in the domain of 2D processing, may also be used for perceiving 3D motion. The question as to how neural circuits implement the differencing operation on eye-specific velocity signals remains open and constitutes a topic of ongoing work.

Relation to past work

Although our results demonstrate that the IOVD cue makes a significant contribution to 3D motion perception that is sometimes superior to the CD cue, it is important to recognize that this role for IOVDs may depend to some extent on the experimental conditions (Regan and Gray 2009). For example, we used a 2AFC direction-discrimination task. We selected this task because it seemed most analogous to a particularly well-studied task in the 2D motion literature (i.e., Newsome and Paré 1988; Watamaniuk et al. 1995), but prior work has (understandably) investigated 3D motion perception using a variety of different tasks, including direction estimation, speed discrimination, judging time to contact, and indicating whether motion through depth is perceived (Brooks and Stone 2006; Harris and Dean 2003; Harris and Watamaniuk 1995; Portfors-Yeomans and Regan 1996). Because each of these tasks might require the observer to rely on and interpret 3D motion signals in different ways—ways that we do not yet fully understand—it is difficult to generalize or compare results across tasks. Indeed, it will be interesting to extend the approach described in this study to these other tasks to build a broader characterization of the relative contributions of the CD and IOVD cues. Although many of these tasks tap important perceptual capacities, we again emphasize that our conclusion that the velocity-based cue plays a major role may reflect the fact that the task and stimuli we chose had strong roots in the literature on both the psychophysics and physiology of 2D motion processing (e.g., Braddick 1974; Newsome and Paré 1988; Perrone and Thiele 2002). Given this constraint, it also had an obvious real-world validity (judging whether something is moving toward or away from your head).

Driven by the goal of maintaining consistency across *FULL*, *CD*, and *IOVD* conditions, we decided to use a single signal plane, which was easily depicted in all cue conditions, salient at high signal strengths, and allowed for straightforward manipulations of both eccentricity and speed. However, it will be important to generalize these results to other stimulus conditions to relate it to a larger body of prior work. Some prior work has used small stimuli relatively near fixation, various types of spatial motion structure (i.e., sinusoidal oscillation, rotation, or oblique trajectories through depth), and element densities ranging from a few percent to complete coverage, all of which could affect the relative contributions of the two cues (e.g., Andrews et al. 2001; Cumming and Parker 1994; Portfors-Yeomans and Regan 1996; Shioiri et al. 2008). Of course this dependence on specific stimulus factors is true whenever one studies a system that can use multiple sources of information. The key point here is that we have found a set of reasonable and simple conditions under which the IOVD cue makes a surprisingly strong contribution to the perception of 3D motion.

We used stimuli that moved across a wide range of constant speeds, consistent with motions of real objects through depth: at our viewing distances, we simulated 3D motions of about 8 to 72 cm/s (the latter corresponds to approximately one and three quarters miles per hour, a reasonable walking speed for a

human). Across this range, we observed large (approximately an order-of-magnitude) changes in overall sensitivity, as well as large relative changes between the *CD* and *IOVD* conditions. These changes in sensitivity suggest that the IOVD cue makes a major contribution to 3D motion perception at ecologically important speeds.

An important prior study concluded that IOVDs did not contribute to 3D motion perception across a very wide range of temporal frequencies (Cumming and Parker 1994). There are several reasons that might explain why we arrived at a starkly complementary conclusion. First, we directly assessed the IOVD contributions using anticorrelated displays, instead of inferring them from the difference between FULL-cue and CD-only displays (although note that, under our experimental conditions, the latter method would still have revealed a large role for IOVDs, as shown in Fig. 8). Importantly, we asked observers to perform a single-interval direction-discrimination task on stimuli moving at a constant speed, which is quite different from the prior study's use of a two-interval signal-present versus signal-absent task on stimuli that oscillated sinusoidally through depth. It is possible that subjects could identify the presence of the signal in this discrimination task by preferentially attending to the slower parts of the sinusoidal oscillation at the extremes of the depth range. Such a strategy could be supported almost exclusively by disparity-based mechanisms and would reveal little about the sensitivity of IOVD versus CD mechanisms.

Despite some significant differences between our experiments and prior ones that arrived at different conclusions, our finding of a central role for IOVDs does not imply that our *CD* stimulus was somehow weak or at a particular disadvantage relative to the other stimuli in our study. In fact, we found that sensitivity in the *CD* condition actually exceeded that in the *FULL* and *IOVD* conditions at the slowest speeds, demonstrating that the *CD* stimulus itself contained strong signals under the viewing conditions that favored CD processing—thus the relative inability of the *CD* condition to account for *FULL* sensitivity at faster speeds almost certainly lies within the visual system. The position-in-depth control experiment lends further support: for the same signal and noise dots, performance on a position-in-depth task was nearly perfect for the *CD* stimuli, but abysmal for the *IOVD* stimuli. Although not conclusive, this is certainly evidence against the notion that CD signals were at a huge disadvantage due to low-level masking.

Moreover, the upper limit of speed sensitivity that we observed is not at odds with some prior studies, most notably that of Cumming and Parker (1994). They collected data at slower speeds, but the sensitivity in their temporally correlated condition (analogous to our *FULL* condition) clearly improves with temporal frequency for both subjects shown, whereas the sensitivity in their dynamic condition (analogous to our *CD* condition) suggests a roll-off around 2 Hz. Although both of their subjects were, in fact, better *overall* in their "CD" condition at the temporal frequencies tested, the difference in sensitivity between the two conditions was also clearly diminishing rapidly with increasing temporal frequency: from their Fig. 3, it is not at all unreasonable to suppose that the sensitivity in their "FULL" condition would begin to exceed that of the "CD" condition had higher temporal frequencies been tested.

In another study, Norcia and Tyler (1984) found that a CD-based depth percept was present $\leq$6 Hz, but they used a square-wave alternation in depth and noted that the percept changed from one of apparent motion (in depth) to one of pulsating semitransparent depth planes as temporal frequency was increased. It is thus unclear what portion of their responses can be attributable to true 3D motion percepts and what portion was due to a modulation of signal strength at different disparities. Moreover, as they themselves noted, their estimate of the temporal resolution of stereoscopic position change was higher than had been reported in previous work (Regan and Beverley 1973; Richards 1972). Overall, we find that the similarity of results to prior work (despite the differences with initial conclusions reported by earlier studies) yields a rather coherent picture of the relative temporal sensitivity of the CD and IOVD cues.

More recent work has also provided evidence for characteristic dependencies of the IOVD cue on speed and eccentricity. Shioiri et al. (2008) reported greater sensitivity to higher temporal frequencies for uncorrelated dot displays (presumably mediated primarily by the IOVD mechanism) than for correlated cyclopean displays (processed exclusively by the CD mechanism). Although observers performed different tasks in the *IOVD* and *CD* conditions (single-interval direction discrimination vs. two-interval signal detection, respectively) and different motion characteristics were present in the two conditions (rotation in depth vs. oscillation in depth, respectively), the general conclusions they arrived at are rather consistent with our speed-tuning observations. Likewise, Brooks and Mather (2000) reported evidence for an IOVD contribution to 3D motion based on manipulations of eccentricity. Reductions in perceived frontoparallel speed at farther eccentricities mirrored reductions in perceived speed of 3D motion, but were relatively independent of eccentricity effects on disparity-based judgments. Such a result is consistent with the robust IOVD contributions across speeds that we observed at middle and far eccentricities.

More generally, our results complement prior attempts to isolate IOVD contributions using a variety of different approaches. Although stimuli containing only CD information without any IOVDs can be straightforwardly generated using one-frame dot lifetimes, a stimulus containing only IOVDs without also containing any potential CD information has not been developed (and may be impossible). Thus prior work has used uncorrelated elements (Brooks 2002a; Shioiri et al. 2000), vertically unmatched strips of opposite motions (Shioiri et al. 2000), or monocular adaptation (Brooks 2002b; Fernandez and Farell 2006). Although details of each of these approaches require careful consideration (e.g., ruling out spurious disparities in uncorrelated stimuli, assessing the effects of optical blur and neural spatial summation in vertically unmatched strip stimuli, and understanding the relationship between monocular adaptation and subsequent dichoptic 3D processing), many of these studies have included careful controls and have begun to form a coherent and compelling case for the importance of IOVDs in 3D motion perception. The overall body of relevant work, including ours, thus encompasses a wide range of tasks and stimuli. Despite this heterogeneity, there is broad agreement that IOVDs do make a distinct contribution to 3D motion perception. Furthermore, they point to the generalization that the CD mechanism is generally low-pass, even if estimates of

the cutoff speed may vary slightly. Moreover, previous studies are generally consistent with the notion that the IOVD cue supports the perception of motion through depth at relatively high speeds, speeds that are beyond the upper limit of dynamic disparity processing. Our ability to compare *FULL*, *IOVD*, and *CD* sensitivities using a common stimulus geometry, task, and sensitivity metric allow us to further suggest that the IOVD cue not only contributes to 3D motion perception, but is in fact dominant in a variety of important conditions.

Implications for future work

At a practical level, our results demonstrate the feasibility of studying the IOVD cue in isolation or, at least, in near-isolation. The use of anticorrelated displays provides a straightforward means for degrading disparity-based signals to reveal the role of the IOVD cue, while maintaining a simple stimulus geometry that supports direct comparison to other 3D motion displays. At a theoretical level, our results provide strong motivation to extend models of motion processing to consider the interocular comparison of monocular velocities. Canonical models of motion processing typically assume that later stages of motion processing operate on generic cyclopean representations (i.e., binocular properties are left unspecified) and thus the representation of eye-specific motions has not been considered (Perrone and Thiele 2002; Rust et al. 2006; Simoncelli and Heeger 1998). Because motion toward or away from the observer typically yields opposite directions of motion in roughly corresponding parts of the two retinae, standard motion mechanisms that involve directional antagonism (motion opponency) need to be modified to be specifically monocular (Majaj et al. 2007). Instead of subtracting these locally opposite directions of motion (for a net result of zero), the visual system must instead extract their signed difference as a cue to 3D velocity.

Furthermore, our results also motivate extensions of models of binocular processing to consider the contributions of monocular motions. Instead of being depicted as an "impurity" relative to CD-only cyclopean stereomotion, our results support a complementary perspective: that the IOVD cue be considered an integral part of seeing motion in depth and that, at least under a wide range of reasonable experimental conditions, the CD cue makes a rather limited contribution. The perception of 3D motion may thus better be thought of as a binocular form of motion processing, rather than as a dynamic form of stereopsis.

GRANTS

This work was supported by National Science Foundation (NSF) CAREER Award BCS-0748413 to A. C. Huk, NSF Grant IIS-0917175 to L. K. Cormack, and Netherlands Organisation for Scientific Research Grant 2006/11353/ALW to B. Rokers.

DISCLOSURES

No conflicts of interest, financial or otherwise, are declared by the authors.

REFERENCES

Andrews TJ, Glennerster A, Parker AJ. Stereoacuity thresholds in the presence of a reference surface. *Vision Res* 41: 3051–3061, 2001.

Blakemore C. The range and scope of binocular depth discrimination in man. *J Physiol* 211: 599–622, 1970.

Braddick O. A short-range process in apparent motion. *Vision Res* 14: 519–527, 1974.

Braddick O. Visual perception. Seeing motion signals in noise. *Curr Biol* 5: 7–9, 1995.

Brainard DH. The Psychophysics Toolbox. *Spat Vis* 10: 433–436, 1997.

Brooks K, Mather G. Perceived speed of motion in depth is reduced in the periphery. *Vision Res* 40: 3507–3516, 2000.

Brooks KR. Interocular velocity difference contributes to stereomotion speed perception. *J Vis* 2: 218–231, 2002a.

Brooks KR. Monocular motion adaptation affects the perceived trajectory of stereomotion. *J Exp Psychol Hum Percept Perform* 28: 1470–1482, 2002b.

Brooks KR, Gillam BJ. The swinging doors of perception: stereomotion without binocular matching. *J Vis* 6: 685–695, 2006.

Brooks KR, Gillam BJ. Stereomotion perception for a monocularly camouflaged stimulus. *J Vis* 7: Art. 1 (1–14), 2007.

Brooks KR, Stone LS. Stereomotion suppression and the perception of speed: accuracy and precision as a function of 3D trajectory. *J Vis* 6: 1214–1223, 2006.

Burr DC, Santoro L. Temporal integration of optic flow, measured by contrast and coherence thresholds. *Vision Res* 41: 1891–1899, 2001.

Cogan AI, Kontsevich LL, Lomakin AJ, Halpern DL, Blake R. Binocular disparity processing with opposite-contrast stimuli. *Perception* 24: 33–47, 1995.

Cormack LK, Stevenson SB, Schor CM. Interocular correlation, luminance contrast and cyclopean processing. *Vision Res* 31: 2195–2207, 1991.

Cormack LK, Stevenson SB, Schor CM. Disparity-tuned channels of the human visual system. *Vis Neurosci* 10: 585–596, 1993.

Cumming BG. The relationship between stereoacuity and stereomotion thresholds. *Perception* 24: 105–114, 1995.

Cumming BG, Parker AJ. Binocular mechanisms for detecting motion-in-depth. *Vision Res* 34: 483–495, 1994.

Cumming BG, Shapiro SE, Parker AJ. Disparity detection in anticorrelated stereograms. *Perception* 27: 1367–1377, 1998.

Fernandez JM, Farell B. Motion in depth from interocular velocity differences revealed by differential motion aftereffect. *Vision Res* 46: 1307–1317, 2006.

Gray R, Regan D. Cyclopean motion perception produced by oscillations of size, disparity and location. *Vision Res* 36: 655–665, 1996.

Harris JM, Dean PJ. Accuracy and precision of binocular 3-D motion perception. *J Exp Psychol Hum Percept Perform* 29: 869–881, 2003.

Harris JM, Nefs H, Grafton CE. Binocular vision and motion-in-depth. *Spat Vis* 21: 531–547, 2008.

Harris JM, Rushton SK. Poor visibility of motion in depth is due to early motion averaging. *Vision Res* 43: 385–392, 2003.

Harris JM, Watamaniuk SN. Speed discrimination of motion-in-depth using binocular cues. *Vision Res* 35: 885–896, 1995.

Julesz B. Binocular depth perception of computer-generated patterns. *Bell Labs Tech J* 39: 1125–1162, 1960.

Julesz B. *Foundations of Cyclopean Perception*. Chicago, IL: Univ. of Chicago Press, 1971, p. xiv.

Kaye M. Stereopsis without binocular correlation. *Vision Res* 18: 1013–1022, 1978.

Lankheet MJ, van Doorn AJ, Bouman MA, van de Grind WA. Motion coherence detection as a function of luminance level in human central vision. *Vision Res* 40: 3599–3611, 2000.

Majaj NJ, Tailby C, Movshon JA. Motion oppenency in area MT of the macaque is mostly monocular. *J Vision* 7: 9.96, 2007.

McKee SP, Nakayama K. The detection of motion in the peripheral visual field. *Vision Res* 24: 25–32, 1984.

Neri P, Parker AJ, Blakemore C. Probing the human stereoscopic system with reverse correlation. *Nature* 401: 695–698, 1999.

Newsome WT, Paré EB. A selective impairment of motion perception following lesions of the middle temporal visual area (MT). *J Neurosci* 8: 2201–2211, 1988.

Norcia AM, Tyler CW. Temporal frequency limits for stereoscopic apparent motion processes. *Vision Res* 24: 395–401, 1984.

Ono H, Barbeito R. Utrocular discrimination is not sufficient for utrocular identification. *Vision Res* 25: 289–299, 1985.

Peng Q, Shi BE. The changing disparity energy model. *Vision Res* 50: 181–192, 2010.

Perrone JA, Thiele A. A model of speed tuning in MT neurons. *Vision Res* 42: 1035–1051, 2002.

Porac C, Coren S. Sighting dominance and utrocular discrimination. *Percept Psychophys* 39: 449–451, 1986.

Portfors-Yeomans CV, Regan D. Cyclopean discrimination thresholds for the direction and speed of motion in depth. *Vision Res* 36: 3265–3279, 1996.

Prince SJD, Cumming BG, Parker AJ. Range and mechanism of encoding of horizontal disparity in macaque V1. *J Neurophysiol* 87: 209–221, 2002.

Regan D, Beverley KI. Some dynamic features of depth perception. *Vision Res* 13: 2369–2379, 1973.

Regan D, Gray R. Binocular processing of motion: some unresolved questions. *Spat Vis* 22: 1–43, 2009.

Richards W. Response functions for sine-and square-wave modulations of disparity. *J Opt Soc Am* 62: 907–911, 1972.

Rokers B, Cormack LK, Huk AC. Strong percepts of motion through depth without strong percepts of position in depth. *J Vis* 8: Art. 6 (1–10), 2008.

Rokers B, Cormack LK, Huk AC. Disparity- and velocity-based signals for three-dimensional motion perception in human MT+. *Nat Neurosci* 12: 1050–1055, 2009.

Rovamo J, Raninen A. Critical flicker frequency and M-scaling of stimulus size and retinal illuminance. *Vision Res* 24: 1127–1131, 1984.

Rust NC, Mante V, Simoncelli EP, Movshon JA. How MT cells analyze the motion of visual patterns. *Nat Neurosci* 9: 1421–1431, 2006.

Scase MO, Braddick OJ, Raymond JE. What is noise for the motion system? *Vision Res* 36: 2579–2586, 1996.

Shioiri S, Nakajima T, Kakehi D, Yaguchi H. Differences in temporal frequency tuning between the two binocular mechanisms for seeing motion in depth. *J Opt Soc Am A* 25: 1574–1585, 2008.

Shioiri S, Saisho H, Yaguchi H. Motion in depth based on inter-ocular velocity differences. *Vision Res* 40: 2565–2572, 2000.

Simoncelli EP, Heeger DJ. A model of neuronal responses in visual area MT. *Vision Res* 38: 743–761, 1998.

Stevenson SB, Cormack LK, Schor CM. The effect of stimulus contrast and interocular correlation on disparity vergence. *Vision Res* 34: 383–396, 1994.

Stevenson SB, Cormack LK, Schor CM, Tyler CW. Disparity tuning in mechanisms of human stereopsis. *Vision Res* 32: 1685–1694, 1992.

Tyler CW. Stereoscopic depth movement: two eyes less sensitive than one. *Science* 174: 958–961, 1971.

Tyler CW. Spatial organization of binocular disparity sensitivity. *Vision Res* 15: 583–590, 1975.

Watamaniuk SN, McKee SP, Grzywacz NM. Detecting a trajectory embedded in random-direction motion noise. *Vision Res* 35: 65–77, 1995.

Watamaniuk SN, Sekuler R, Williams DW. Direction perception in complex dynamic displays: the integration of direction information. *Vision Res* 29: 47–59, 1989.

Watanabe Y, Kezuka T, Harasawa K, Usui M, Yaguchi H, Shioiri S. A new method for assessing motion-in-depth perception in strabismic patients. *Br J Ophthalmol* 92: 47–50, 2008.

Westheimer G, Truong TT. Target crowding in foveal and peripheral stereoacuity. *Am J Optom Physiol Opt* 65: 395–399, 1988.

Wright MJ. Spatiotemporal properties of grating motion detection in the center and the periphery of the visual field. *J Opt Soc Am A* 4: 1627–1633, 1987.